



A high step up Application of Stand-Alone Photovoltaic and Battery Power Systems

¹L S N Sairam,²Ch. Vinod Kumar

¹M.tech(Research scholar),²Associate Professor in Dept. of Electronics And Communication Engineering
Kakinada Institute Of Engineering And Technology-II
Yanam Road , Korangi-533461

Abstract

A three-port dc–dc converter integrating photovoltaic (PV) and battery power for high step-up applications is proposed in this paper. The topology includes five power switches, two coupled inductors, and two active-clamp circuits. The coupled inductors are used to achieve high step-up voltage gain and to reduce the voltage stress of input side switches. Two sets of active-clamp circuits are used to recycle the energy stored in the leakage inductors and to improve the system efficiency. The operation mode does not need to be changed when a transition between charging and discharging occurs. Moreover, tracking maximum power point of the PV source and regulating the output voltage can be operated simultaneously during charging/discharging transitions. As long as the sun irradiation level is not too low, the maximum power point tracking (MPPT) algorithm will be disabled only when the battery charging voltage is too high. Therefore, the control scheme of the proposed converter provides maximum utilization of PV power most of the time. As a result, the proposed converter has merits of high boosting level, reduced number of devices, and simple control strategy.

I. Introduction

Integrated multiport converters for interfacing several power sources and storage devices are widely used in recent years. Instead of using individual power electronic converters for each of the energy sources, multiport converters have the advantages including less components, lower cost, more compact size, and better dynamic performance. In many cases, at least one energy storage device should be incorporated. For example, in the electric vehicle application, the regenerative energy occurs during acceleration or startup. Therefore, it is very important for the port connected to the energy storage to allow bidirectional power flow.

Various kinds of topologies have been proposed due to the advantages of multiport

converters. The combination strategies for the multiport converter include sharing switches, capacitors, inductors, or magnetic cores [1]. One could select a proper topology by considering many aspects such as cost, reliability, and flexibility depending on the applications. An application of hybrid energy supply using renewable energy sources and storage devices is shown in Fig. 1. The dc microgrid enabled by the solid-state transformer (SST) in the Future Renewable Electric Energy Delivery and Management System (FREEDM System) integrates various distributed renewable energy resources (DRERs) and distributed energy storage devices (DESDs) [2]. For instance, if solar power is selected as the renewable energy source and battery as the storage device, the battery can either supply the load with the solar energy at the same time or store the excess power from the solar panels for backup use. Therefore, the bidirectional power path must be provided for the battery port. The dc–dc converters interfacing the DRERs or DESDs are expected to have relative high voltage conversion ratios since the dc bus of the FREEDM system is 380 V. It is studied that for the dc–dc converters connected to the solar panels, voltage gain extension cells such as coupled inductors, transformers, and switched capacitors are often employed to achieve high voltage conversion ratios [3]. By utilizing the voltage gain extension cells, the extreme duty cycles that exist in typical boost converters can be avoided and the voltage stress on switches can be reduced. Thus, power switches with lower voltage rating and lower turn-on resistance can be chosen for the converters to reduce conduction losses.

A converter using coupled inductors is relatively better than isolation transformers since the coupled inductors have simpler winding structure and lower conduction loss [4]. However, the leakage inductors of the coupled inductors will consume significant energy for a large winding ratio. In such case, the voltage stress and the loss of the switches will both be increased. A boost converter with

coupled inductor and active-clamp circuit is proposed in [4]. This boost converter can yield a high step-up voltage gain, reduce the voltage stress on switches, and recycle the energy in the leakage inductor.

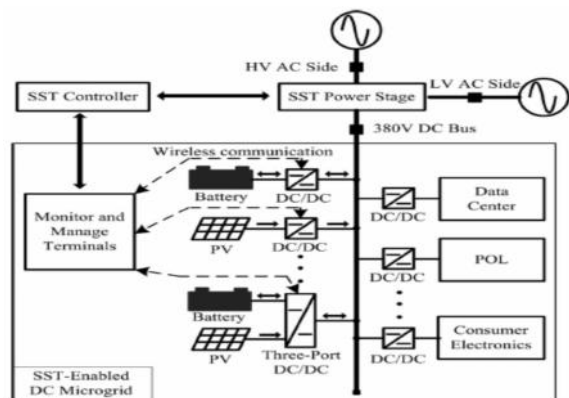


Fig. 1. Part of the FREEDM system diagram showing an SST-enabled DCmicro grid.

Many multiport converter topologies have been presented in the literature and can be roughly divided into two categories. One is nonisolated type [5]–[13]: the nonisolated converters are usually derived from the typical buck, boost, or buck-boost topologies and are more compact in size. The other is isolated type [14]–[24]: the isolated converters using bridge topologies and multiwinding transformers to match wide input voltage ranges.

Principle Of Operation

This section introduces the topology of proposed nonisolated three-port dc–dc converter, as illustrated in Fig. 2. The converter is composed of two main switches $S1$ and $S2$ for the battery and PV port. Synchronous switch $S3$ is driven complementarily to $S1$ such that bidirectional power flow for the battery port can be achieved. Two coupled inductors with winding ratios $n1$ and $n2$ are used as voltage gain extension cells. Two sets of active-clamp circuits formed by $S4$, $Lk1$, $Cc1$ and $S5$, $Lk2$, $Cc2$ are used to recycle the leakage energy. $Lk1$ and $Lk2$ are both composed of a small leakage inductor from the coupled inductor and an external leakage inductor. Two independent control variables, duty cycles $d1$ and $d2$, allow the control over two ports of the converter, while the third port is for the power balance. The fixed-frequency driving signals of the auxiliary switches $S3$ and $S4$ are complementary to primary switch $S1$. Again, $S3$ provides a bidirectional path for the battery port. Similarly, $S5$ is driven in a complementary manner to $S2$. An 180 phase shift is applied between the driving signals of $S1$ and $S2$. There are four operation periods based on the available solar power. First, the

sun is in the eclipse stage and the solar irradiation is either unavailable or very low. This operation period is defined as period 1, and the battery will serve as the main power source. As the sun starts to shine and the initial solar irradiation is enough for supplying part of the load demand, the operation period is changed to period 2. The load is supplied by both solar and battery power in this period. For period 3, the increasing irradiation makes the solar power larger than the load demand. The battery will preserve extra solar power for backup use. During period 4, the charging voltage of the battery reaches the preset level and should be limited to prevent overcharging. According to the solar irradiation and the load demand, the proposed three-port converter can be operated under two modes. In the battery balance mode (mode 1), maximum power point tracking (MPPT) is always operated for the PV port to draw maximum power from the solar panels. The battery port will maintain the power balance by storing the unconsumed solar power during light-load condition or providing the power deficit during heavy-load condition.

Simulation Results

In Fig. 2, the sun radiation is in period 1. For the first 40 s, there is very little sunlight, so the MPPT is performed. However, once the level is too low or not available, MPPT is then disabled and the battery will become the only power source to supply the load. In Fig. 3(a) and (b), the sun irradiation is in period 2. The solar port is operated under MPPT and the battery port is discharged to supply part of the load. As the irradiation increases, the PV port will generate more power than the battery port. The increasing sun irradiation reaches period 3 in Fig. 4. The power generated from the PV port is now larger than the load demand, so the battery port should be charged to store additional power. Although the batteries are charged, the charging voltage is not high enough to trigger the BVC loop. Thus, the solar panels still work under MPPT. As shown in Fig. 14, the maximum charging voltage for the batteries is reached in period 4.

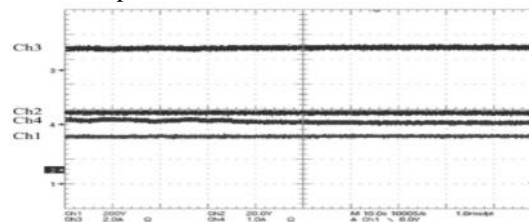


Fig. 2. Measured waveforms of mode operation in period 1 ($R = 3030$, Ch1: V_o , Ch2: V_b , Ch3: I_b , Ch4: I_{pv}).

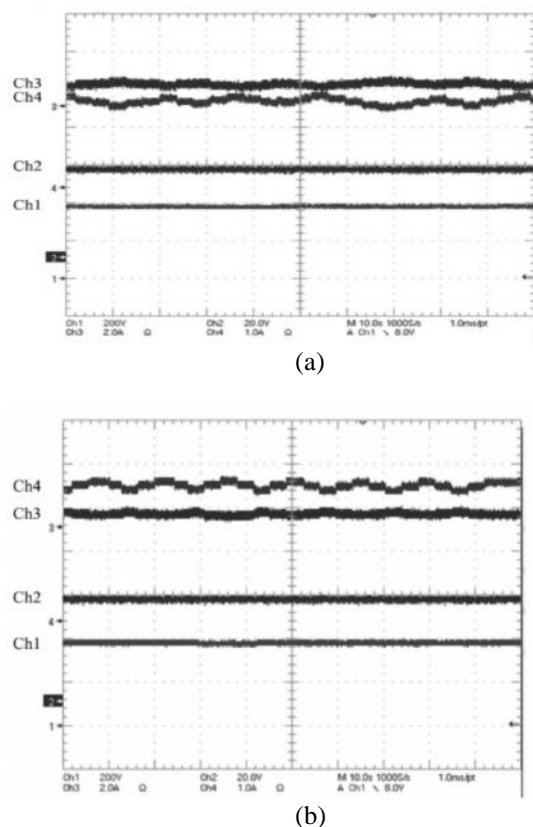


Fig. 3. Measured waveforms of mode operation in period 2. (a) Lower solar irradiation level. (b) Higher solar irradiation level ($R = 1204$, Ch1: V_o , Ch2: V_b , Ch3: I_b , Ch4: I_{pv}).

The BVC loop is then active to regulate the charging voltage and the MPPT is disabled. At the beginning of Fig. 15, the load demand is set as 120 W ($R = 1204$), the solar port is generating its maximum power and the deficit is provided by the battery port. At the time $t = 32$ s, load demand is decreased to 72 W ($R = 2000$), which is lower than the power generated from the solar panels. The maximum solar power is still drawn from the panel after the load change and the batteries are charged by the additional solar power. It is observed that the current ripple of the battery is larger at the boundary of charging and discharging operations. When $t = 58$ s, the load is switched back to 120W, so the batteries are discharged again. It can be observed that the solar port works under MPPT as long as the battery voltage is not too high. The transitions of the battery between charging and discharging are smooth and the operation mode does not need to be changed.

It should be noted that even during the load change, MPPT is achieved and the output voltage is well regulated. This is one of the important features

of three-port converters since MPPT and load regulation could not be maintained simultaneously for typical two-port converters [22].

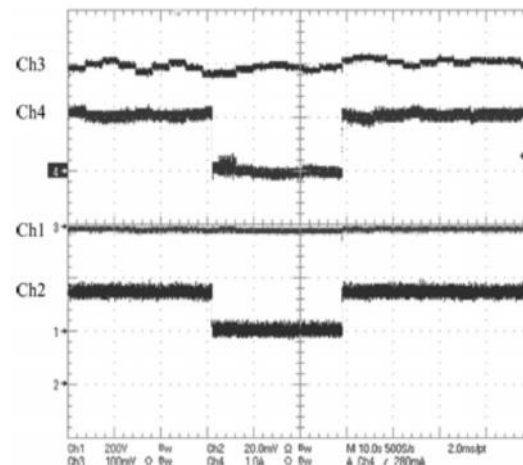


Fig. 4. Measured waveforms of load step response under SVC (Ch1: V_o , Ch2: I_o , Ch3: I_{pv} , Ch4: I_b).

Fig. 5(a) shows mode transition from SVC (mode 1: MPPT, $R = 900$) to BVC (mode 2: Battery voltage regulation, $R = 3600$) when the maximum charging voltage is reached. The PV port is operated under MPPT at the beginning to generate maximum solar power and the battery is discharged to share part of the load demand. It is noted that in mode 1, sometimes the solar power is slightly larger than the load demand; therefore, the batteries are temporally charged. The battery voltage in this case is clearly higher than discharging situation. However, the charging voltage during this short period is not high enough, so the converter is still operated in mode 1. When a load change (from 80% to 20%) happened at $t = 50$ s, the battery is suddenly charged with a large current and the battery voltage is then increased dramatically. When the charging voltage is higher than the maximum setting, the operation mode is switched to mode 2 immediately to regulate the battery voltage and prevent overcharging.

It can be seen that in mode 2, the solar panel is no longer operated around the maximum power point but the right side of it. Fig. 5(b) shows the transition from mode 2 to mode 1 when the load is suddenly increased. The SVC will take over the control on the PV port since the maximum setting of the battery voltage could not be met. Similarly, sometimes the batteries could be slightly charged according to the intensity of solar irradiation. Again, no matter what mode is operated for the PV port, the output voltage will be always regulated at 380 V.

Conclusion And Future Work

A high step-up three-port DC–DC converter for stand-alone power systems is proposed to integrate solar and battery power. In the proposed topology, two coupled inductors are employed as voltage gain extension cells for high voltage output applications.

Discussion from control viewpoints including moving the effect of RHP-zero to particular output, limitations on sensitivity of the system, tradeoffs in the feedback controller design, and implementation of an improved decoupling method should be presented in our future work.

References

- [1] S. H. Choung and A. Kwasinski, "Multiple-input DC-DC converter topologies comparison," in *Proc. 34th Annu. Conf. IEEE Ind. Electron.*, 2008, pp. 2359–2364.
- [2] A. Huang, "FREEDM system—a vision for the future grid," in *Proc. IEEE Power Energy Soc. Gen. Meet.*, 2010, pp. 1–4.
- [3] W. Li and X. He, "Review of nonisolated high-step-up DC/DC converters in photovoltaic grid-connected applications," *IEEE Trans. Ind. Electron.*, vol. 58, no. 4, pp. 1239–1250, Apr. 2011.
- [4] T.-F. Wu, Y.-S. Lai, J.-C. Hung, and Y.-M. Chen, "Boost converter with coupled inductors and buck-boost type of active clamp," *IEEE Trans. Ind. Electron.*, vol. 55, no. 1, pp. 154–162, Jan. 2008.
- [5] W. G. Imes and F. D. Rodriguez, "A two-input tri-state converter for spacecraft power conditioning," in *Proc. AIAA Int. Energy Convers. Eng. Conf.*, 1994, pp. 163–168.
- [6] F. D. Rodriguez and W. G. Imes, "Analysis and modeling of a two input DC/DC converter with two controlled variables and four switched networks," in *Proc. AIAA Int. Energy Conf.*, 1994, pp. 163–168.
- [7] B. G. Dobbs and P. L. Chapman, "A multiple-input DC–DC converter topology," *IEEE Power Electron. Lett.*, vol. 1, no. 1, pp. 6–9, Mar. 2003.
- [8] R. J. Wai, Ch. Y. Lin, J. J. Liaw, and Y. R. Chang, "Newly designed ZVS multi-input converter," *IEEE Trans. Ind. Electron.*, vol. 58, no. 2, pp. 555–566, Feb. 2011.
- [9] L. Solero, A. Lidozzi, and J. A. Pomilio, "Design of multiple-input power converter for hybrid vehicles," in *Proc. IEEE Appl. Power Electron. Conf.*, 2004, pp. 1145–1151.
- [10] F. Nejabatkhah, S. Danyali, S. H. Hosseini, M. Sabahi, and S. M. Niapour, "Modeling and control of a new three-input DC-DC boost converter for hybrid PV/FC/battery power system," *IEEE Trans. Power Electron.*, vol. 23, no. 2, pp. 782–792, Mar. 2008.
- [11] J. Jung and A. Kwasinski, "A multiple-input SEPIC with a bi-directional input for modular distributed generation and energy storage integration," in *Proc. IEEE Appl. Power Electron. Conf.*, 2011, pp. 28–34.
- [12] G.-J. Su and F. Z. Peng, "A low cost, triple-voltage bus DC–DC converter for automotive applications," in *Proc. IEEE Appl. Power Electron. Conf.*, 2005, pp. 1015–1021.
- [13] A. Kwasinski, "Identification of feasible topologies for multiple-input DCDC converters," *IEEE Trans. Power Electron.*, vol. 24, no. 3, pp. 856–861, Mar. 2009.
- [14] S. Yu and A. Kwasinski, "Analysis of a soft-switching technique for isolated time-sharing multiple-input converters," in *Proc. IEEE Appl. Power Electron. Conf.*, 2012, pp. 844–851.
- [15] D. Liu and H. Li, "A ZVS bi-directional DC–DC converter for multiple energy storage elements," *IEEE Trans. Power Electron.*, vol. 21, no. 5, pp. 1513–1517, Sep. 2006.
- [16] H. Tao, A. Kotsopoulos, J. L. Duarte, and M. A. M. Hendrix, "Triple half-bridge bidirectional converter controlled by phase shift and PWM," in *Proc. IEEE Appl. Power Electron. Conf.*, Mar. 2006, pp. 1256–1262.
- [17] L. Wang, Z. Wang, and H. Li, "Asymmetrical duty cycle control and decoupled power flow design of a three-port bidirectional DC-DC converter for fuel cell vehicle application?," *IEEE Trans. Power Electron.*, vol. 27, no. 2, pp. 891–903, Feb. 2012.
- [18] Y.-M. Chen, Y.-C. Liu, and F.-Y. Wu, "Multi-input DC/DC converter based on the multiwinding transformer for renewable energy applications," *IEEE Trans. Ind. Appl.*, vol. 38, no. 4, pp. 1096–1104, Jul./Aug. 2002.
- [19] H. Tao, A. Kotsopoulos, J. L. Duarte, and M. A. M. Hendrix, "Transformer coupled multiport ZVS bidirectional DC–DC converter with wide input range," *IEEE Trans. Power Electron.*, vol. 23, no. 2, pp. 771–781, Mar. 2008.
- [20] C. Zhao, S. D. Round, and J. W. Kolar, "An isolated three-port bidirectional DC–DC converter with decoupled power flow management," *IEEE Trans. Power Electron.*, vol. 23, no. 5, pp. 2443–2453, Sep. 2008.
- [21] H. Krishnaswami and N. Mohan, "Three-port series resonant DC-DC converter to interface renewable energy sources with bidirectional load and energy storage ports," *IEEE Trans. Power Electron.*, vol. 24, no. 10, pp. 2289–2297, Oct. 2009.
- [22] H. Al-Atrash, F. Tian, and I. Batarseh, "Trimodal half-bridge converter topology for three-port interface," *IEEE Trans. Power Electron.*, vol. 22, no. 1, pp. 341–345, Jan. 2007.